1   Pneumolysin is responsible for differential gene expression and modifications in the

2   epigenetic landscape of primary monocyte derived macrophages.

3

4   J. Cole[1,2,3,4], A. Angyal[1], R. D.Emes[5], T.J. Mitchell[7], M.J. Dickman[4], D.H. Dockrell[8]

5   1) Department of Infection, immunity & Cardiovascular Diseases, University of

6   Sheffield,

7   2) Sheffield Teaching Hospitals NHS FT

8   3) The Florey Institute, University of Sheffield

9   4) Department of Chemical & Biological Engineering, University of Sheffield,

10   5) Advanced Data Analysis centre, University of Nottingham,

11   6) School of Veterinary Medicine and Science. University of Nottingham,

12   7) Institute of Microbiology and Infection, University of Birmingham

13   8) MRC Centre for Inflammation Research, University of Edinburgh

14

15

16 **Abstract:**

17 Epigenetic modifications regulate gene expression in the host response to a

18 diverse range of pathogens. The extent and consequences of epigenetic modification

19 during macrophage responses to *Streptococcus pneumoniae,* and the role of

20 pneumolysin, a key *Streptococcus pneumoniae* virulence factor, in influencing these

21 responses, are currently unknown. To investigate this, we infected human monocyte

22 derived macrophages (MDMs) with *Streptococcus pneumoniae* and addressed

23 whether pneumolysin altered the epigenetic landscape and the associated acute

24 macrophage transcriptional response using a combined transcriptomic and proteomic

25 approach. Transcriptomic analysis identified 503 genes that were differentially

26 expressed in a pneumolysin-dependent manner in these samples. Pathway analysis

27 highlighted the involvement of transcriptional responses to core innate responses to

28 pneumococci including modules associated with metabolic pathways activated in

29 response to infection, oxidative stress responses and NFκB, NOD-like receptor and

30 TNF signalling pathways. Quantitative proteomic analysis confirmed pneumolysin-

31 regulated protein expression, early after bacterial challenge, in representative

32 transcriptional modules associated with innate immune responses. In parallel,

33 quantitative mass spectrometry identified global changes in the relative abundance of

34 histone post translational modifications (PTMs) upon pneumococcal challenge. We

35 identified an increase in the relative abundance of H3K4me1, H4K16ac and a

36 decrease in H3K9me2 and H3K79me2 in a PLY-dependent fashion. We confirmed

37 that pneumolysin blunted early transcriptional responses involving TNF-α and IL-6

38 expression. Vorinostat, a histone deacetylase inhibitor, similarly downregulated TNF

39 production, reprising the pattern observed with pneumolysin. In conclusion,

40 widespread changes in the macrophage transcriptional response are regulated by

41   pneumolysin and are associated with global changes in histone PTMs. Modulating

42   histone PTMs can reverse pneumolysin-associated transcriptional changes

43   influencing innate immune responses, suggesting that epigenetic modification by

44   pneumolysin plays a role in dampening the innate responses to pneumococci.

45

46   **Author summary:**

47   Pneumolysin is a toxin that contributes to how *Streptococcus pneumoniae*, the

48   leading cause of pneumonia, causes disease. In this study, the toxin alters gene

49   expression in immune cells called macrophages, one of the first lines of defence

50   against bacteria at sites of infection. Modulation involved multiple immune responses,

51   including generation of chemical signals coordinating responses in immune cells

52   termed cytokines. In addition, changes were observed in histone proteins that are

53   involved in controlling gene expression in the cell. Pneumolysin reduced early

54   production of the cytokine TNF-α and a medicine vorinostat that modifies these

55   'epigenetic' histone modifications had a similar affect, suggesting epigenetic

56   mechanisms contribute to the ability of pneumolysin to reduce immune responses.

57

Introduction:

Pneumolysin (PLY) is one of the key virulence factors of *S. pneumoniae* (the pneumococcus), the leading cause of community-acquired pneumonia (Kadioglu et al. 2008) and is present in the majority of clinical isolates causing invasive pneumococcal disease (IPD) (Gray, Converse, and Dillon 1980; D.-K. Hu et al. 2015). Pneumolysin is a cholesterol-dependent cytolysin and part of a family of toxins expressed in Gram-positive bacteria (Tweten 2005). It is a 53 kDa protein that contains four domains (Walker et al. 1987). One mechanism of action is through pore formation (van Pee et al. 2017) but increasingly it is recognized to mediate additional actions independent of the ability to form pores (Bewley et al. 2014).

In murine models of bacteraemia PLY sufficient mutants are associated with increased lethality compared to PLY deficient mutants, linking the toxin to virulence (Benton, Everson, and Briles 1995). Furthermore, the transmission of *S. pneumoniae* between hosts has been linked to the presence of inflammation in the nasopharynx and pneumolysin has been shown to promote inflammation, increase transmission and foster the survival *ex vivo* of *S. pneumoniae* (Zafar et al. 2017). It has been also suggested that pneumolysin facilitates blood stream invasion by *S. pneumoniae* (D.-K. Hu et al. 2015). This highlights its importance as a key virulence factor of *S. pneumoniae* due to its role in the transmission of *S. pneumoniae* between hosts, in the progression from nasopharyngeal colonisation to invasive pneumococcal disease, the stimulation of inflammation and its cytotoxic effects (Kadioglu et al. 2008).

Pneumolysin has been shown to alter a variety of immune responses. For example it has been demonstrated to both activate the classical complement pathway (Paton, Rowan-Kelly, and Ferrante 1984) as well as play a role in complement evasion (Quin, Moore, and McDaniel 2007). Pneumolysin has been associated with stimulation

83   of NRLP3 and potentially other inflammasome components (McNeela et al. 2010; R.

84   Fang et al. 2011). In human monocytes it is associated with production of tumour

85   necrosis factor alpha (TNF-α) and interleukin (IL-)1β (Houldsworth, Andrew, and

86   Mitchell 1994). Pneumolysin has been shown to be responsible for the differential

87   expression of multiple genes in undifferentiated THP-1 cells, a monocytic cell line,

88   (Rogers et al. 2003) but its impact on gene expression in primary macrophages has

89   not been established in detail. More recently, pneumolysin has been shown to bind

90   the mannose receptor C type 1 in mouse alveolar macrophages leading to diminished

91   pro-inflammatory cytokine release and enhanced bacterial survival (Subramanian et

92   al. 2019).

93   The subversion of the host immune system is one of the key components of

94   bacterial pathogenesis. Microorganisms can highjack host gene expression to their

95   benefit (Eskandarian et al. 2013; Hamon et al. 2007; Rolando et al. 2013). Epigenetic

96   mechanisms such as histone post-translational modifications (PTMs) have been

97   shown to regulate gene transcription (Berger 2007; Jenuwein and Allis 2001).

98   Moreover, they can be modulated by a number of different bacterial components (Cole

99   et al. 2016). Experiments using both *Legionella pneumophila* (Rolando et al. 2013),

100   and *Listeria monocytogenes* (Eskandarian et al. 2013) have shown that bacterial

101   interaction with the THP-1 monocytic cell line also modifies histone PTMs. In the case

102   of *Listeria monocytogenes*, Listeriolysin O, a pore-forming cytolysin similar to PLY, is

103   secreted causing dephosphorylation at serine 10 of histone H3 and reduction in the

104   levels of acetylated H4 in THP-1 cells. In HeLa cells these changes altered the

105   transcriptional profile, which was associated with a decrease in IL-6 and other genes

106   involved in innate immune responses (Hamon et al. 2007). This supports the

107 hypothesis that bacteria alter the epigenetic profile of the host cell as a strategy for

108 immune subversion, limiting the inflammatory response to increase their survival.

109   The consequences of epigenetic changes during acute bacterial infections are,

110 however, not fully understood. The aim of this study was to investigate the

111 consequences and mechanism underpinning the ability of pneumolysin to modulate

112 translational responses to *S. pneumoniae* using primary human macrophages. We

113 found that pneumolysin modulates a broad range of immune transcriptional responses

114 in macrophages and differential protein expression analysis also confirmed changes

115 in key transcriptional modules. Moreover, we identified global changes in the

116 abundance of histone PTMs in MDMs in a pneumolysin dependent manner. We

117 illustrate that one key pneumolysin-regulated immune response, early TNF-α

118 production is also altered by chemical manipulation of histone PTMs.

119

6

120 **Results:**

121 **Pneumolysin shapes the macrophage transcriptome in response to**
122 **pneumococci.**

123
124   Transcriptional responses to Gram-positive bacteria occur rapidly and are well

125 developed after three hours of bacterial challenge (Hamon et al. 2007)(Rogers et al.

126 2003). Therefore, we initially analyzed transcriptional changes in monocyte-derived

127 macrophages (MDMs) three hours after bacterial challenge with either wild-type or a

128 pneumolysin deficient (∆PLY) strains. We confirmed that intracellular viability of

129 pneumococci was equivalent at this time between wild-type and ∆PLY strains (Fig S1),

130 thereby excluding potential confounding by different levels of vita-pathogen-

131 associated molecular pattern (Sander et al. 2011).

132   We identified 1872 probe-sets that were differentially expressed in response to

133 bacterial challenge with either strain (F value <0.05) and 1553 after multiple test

134 correction false discovery rate (FDR <0.05). Next, we calculated moderated t tests for

135 each infection, as shown in the Volcano plots in Figure 1. The analysis identified 503

136 probe-sets which are differentially expressed in a pneumolysin-dependent manner

137 and 234 in an independent manner (summarised Fig S2). To provide further insight

138 into the pneumolysin-dependent differential gene expression in MDMs we undertook

139 pathway analysis of the differentially expressed genes.

140

141 **Pathway analysis of differentially expressed genes:**

142   Gene Ontology (GO) pathway analysis demonstrated that the top ten enriched

143 terms in the pneumolysin-dependent differentially expressed genes were

144 predominantly related to cell metabolism (Fig S3). However, there were also a number

145 of terms relating to cellular responses to "stress" (17 in the *S. pneumoniae* challenge

146 and 15 in the ΔPLY mutant) and in particular to oxidative stress responses. The

147 volcano plots for the differentially expressed genes belonging to the GO term for

148 oxidative stress response were plotted for each strain (Fig 2). These results

149 highlighted that the differentially expressed genes were predominantly upregulated.

150 Moreover, the TNF, heme oxygenase 1 (HMOX1) and prostaglandin-endoperoxide

151 synthase 2 (PTGS2) genes were strongly upregulated.

152   In addition to performing Gene ontology analysis we also analysed the

153 differentially expressed genes using eXploring Genomic Relations (XGR) which

154 performs hypergeometric enrichment analysis with background correction using the

155 expression of monocyte derived macrophage cells to give a more cell type specific

156 analysis. Canonical pathway analysis was performed for genes whose expression was

157 upregulated in response to challenge with *S. pneumoniae* (adjusted p value <0.05).

158 This revealed 36 over-represented pathways (Table S1). Importantly this

159 demonstrated that both the TNF and the NFκB signalling pathways were enriched.

160 Analysis of the 2-fold downregulated terms did not reveal any enriched canonical

161 pathways.

162   The analysis of the differentially expressed genes whose expression was up-

163 regulated by greater than 2-fold in response to challenge with the ΔPLY mutant also

164 revealed that the pathways for TNF, NFκB and CD40 signalling were significantly over-

165 represented (Table S2). This highlights the importance of these pathways in the

166 response to bacterial challenge. It also suggests that the increase in pro-inflammatory

167 signals being released in particular TNF is independent of PLY. Of note, we observed

168 a 6-fold increase in the TNF mRNA in response to ΔPLY but only 4-fold increase in

169 response to the parent strain (Fig 2).

170   **Label-free quantitative proteomic analysis:**

171   Having established that there was a transcriptional difference in the host cell

172   response following challenge with *S. pneumoniae* or ΔPLY, further studies were

173   performed to examine the effects of *S. pneumoniae* on the proteome of MDMs.

174   Label free quantitative mass spectrometry was used to identify differentially

175   expressed proteins following challenge with *S. pneumoniae* or ΔPLY. We identified

176   1807 proteins in samples challenged with *S. pneumoniae* and 1862 in those

177   challenged with ΔPLY. On average we identified 1812 proteins in each of the 12

178   samples from 4 biological replicates that we analysed. Of these, we identified 32 that

179   were differentially expressed between the three conditions with an F statistic value of

180   less than 0.05 (summarised in Table 1). The results show that 16 proteins are

181   differentially expressed in response to infections with *S pneumoniae,* and 22 in

182   response to ΔPLY. Eight proteins were differentially expressed in a pneumolysin-

183   dependent manner, these included serine / threonine protein kinase 1, also known as

184   the oxidative stress response 1 protein (OXSR1) and Ubiquitin domain-containing

185   protein 1 / 2 (UBTD2), and 9 were common to both bacterial strains, including Galectin

186   3 binding protein which is involved in the host immune responses (Breuilh et al. 2007)

187   and the 26S proteasome non-ATPase regulatory subunit 5 (PSMD5). Several of the

188   differentially expressed proteins identified such as PSMD5, UBTD2 and Ubiquitin

189   conjugation factor E4 A (UBE4A) are involved in protein turn-over involving a number

190   of pathways known to be important in the regulation of host immune responses (H. Hu

191   and Sun 2016).

192

193

194

195 Table 1: Differentially expressed proteins at 6 h following challenge with *S pneumoniae*

196 or ΔPLY.

Majority Protien ID	MI vs *S pneumoniae*			MI vs ΔPLY			protein name	Gene name
	logFC	P.Value	adj.P.Val	logFC	P.Value	adj.P.Val		
P23219;A0A087X296	-2.83E+00	1.96E-03	6.42E-03	-1.67E+00	1.70E-02	2.60E-02	Prostaglandin G/H synthase 1	PTGS1
O95747;C9JIG9	-2.36E+00	2.39E-05	3.82E-04	-1.03E+00	4.02E-02	5.59E-02	Serine/threonine-protein kinase OSR1	OXSR1
P51531;A0A0U1RQZ9;F6VDE0;Q9HBD4;A0A0A0MT49;P51532;A0A0U1RRD6;A0A0U1RRF8;A0A0A0MSS5;F6UH26;A0A0U1RQU0;A0A0U1RR09;F6XE55;A0A0U1RQW7;A0A0U1RRN2;B1ALG1;A0A0U1RR83;A0A0U1RQX3;F6T8Q0;B1ALG2;A0A0U1RR26;A0A0U1RRG6;B4DNT1;B1ALF6	-3.69E+00	3.61E-05	3.85E-04	-5.99E-01	4.37E-01	4.99E-01	Probable global transcription activator SNF2L2 / Transcription activator BRG1	SMARCA2 / SMARCA4
Q08380;K7EJY8;K7ESM3;K7EKQ5;K7EP36	-2.36E+00	1.57E-04	1.26E-03	-1.94E+00	1.30E-03	2.96E-03	Galectin-3-binding protein	LGALS3BP
Q9HAC8;Q8WUN7	2.84E+00	3.87E-04	2.48E-03	6.83E-01	2.49E-01	2.95E-01	Ubiquitin domain-containing protein 1 / 2	UBTD2
P36871	-2.19E+00	5.77E-03	1.42E-02	-2.69E+00	1.02E-04	8.14E-04	Phosphoglucomutase-1	PGM1
Q709C8	-1.83E+00	2.00E-03	6.42E-03	-2.06E+00	1.78E-04	1.04E-03	Vacuolar protein sorting-associated protein 13C	VPS13C
M0R300;M0R0P8;Q13459	-1.27E+00	2.17E-02	4.09E-02	-2.05E+00	6.71E-03	1.13E-02	Unconventional myosin-Ixb	MYOB9B
A0A0C4DG89;Q7L014;D6RJA6	1.69E+00	1.83E-03	6.42E-03	6.49E-01	1.74E-01	2.15E-01	Probable ATP-dependent RNA helicase DDX46	DDX46
P46087	1.62E+00	1.39E-03	6.42E-03	6.09E-02	9.07E-01	9.32E-01	Probable 28S rRNA (cytosine(4447)-C(5))-methyltransferase	NOP2
O60826	2.54E+00	4.21E-03	1.23E-02	9.88E-01	1.50E-01	1.92E-01	Coiled-coil domain-containing protein 22	CCDC22
Q9Y5X2	1.63E+00	1.18E-02	2.47E-02	-1.22E+00	2.31E-02	3.36E-02	Sorting nexin-8	SNX8

Q5U5X0	1.66E+00	4.79E-03	1.28E-02	1.47E+00	5.25E-03	9.57E-03	Complex III assembly factor LYRM7	LYRM7
R4GMN1;Q8NHP6	-1.29E+00	6.85E-03	1.57E-02	-4.13E-02	9.32E-01	9.32E-01	Motile sperm domain-containing protein 2	MOSPD2
A0A087WUZ3;Q01082	2.52E+00	1.73E-03	6.42E-03	2.02E+00	2.02E-03	4.05E-03	Spectrin beta chain, non-erythrocytic 1	SPTBN1
O95336;M0R261	-1.18E+00	1.23E-02	2.47E-02	-6.15E-02	8.98E-01	9.32E-01	6-phosphoglucono lactonase	PGLS
Q16401;F2Z3J2	2.76E+00	1.92E-06	6.14E-05	1.90E+00	6.73E-04	1.66E-03	26S proteasome non-ATPase regulatory subunit 5	PSMD5
Q14139	-1.69E+00	5.47E-02	8.34E-02	3.92E+00	7.24E-05	7.72E-04	Ubiquitin conjugation factor E4 A	UBE4A
O95865;A0A140T971;Q5SSV3;Q5SRR8	-1.48E+00	3.31E-02	5.88E-02	-2.13E+00	2.95E-04	1.09E-03	N(G),N(G)-dimethylarginine dimethylaminohydrolase 2	DDAH2
P26639	-1.42E+00	4.11E-02	6.93E-02	-2.12E+00	5.38E-03	9.57E-03	Threonine--tRNA ligase, cytoplasmic	TARS
Q9BXW7	-8.74E-01	2.29E-01	2.62E-01	-2.79E+00	2.39E-04	1.09E-03	Haloacid dehalogenase-like hydrolase domain-containing 5	HDHD5
F8W031;F8VXJ7;Q9Y2B0;F8W1K5	-8.82E-01	5.89E-02	8.56E-02	6.65E-01	1.50E-01	1.92E-01	Protein canopy homolog 2	CNPY2
H0Y8C3;Q9NZJ7	-8.67E-01	8.03E-02	1.08E-01	-2.88E+00	2.34E-05	3.75E-04	Mitochondrial carrier homolog 1	MTCH1
Q92616	-7.39E-01	1.55E-01	1.91E-01	-1.79E+00	6.15E-04	1.66E-03	eIF-2-alpha kinase activator GCN1	GCN1
O00115;K7ENE5	-6.51E-01	9.23E-02	1.18E-01	8.86E-02	8.15E-01	9.00E-01	Deoxyribonuclease-2-alpha	DNASE2
H0Y8X4;O43598	-2.52E-01	7.29E-01	7.52E-01	-2.74E+00	3.39E-04	1.09E-03	2'-deoxynucleoside 5'-phosphate N-hydrolase 1	DNPH1
Q92508	2.29E-01	7.61E-01	7.61E-01	-2.36E+00	1.96E-04	1.04E-03	Piezo-type mechanosensitive ion channel component 1	PIEZO1
E9PF10;O75694	3.86E-01	5.89E-01	6.29E-01	2.01E+00	1.53E-03	3.27E-03	Nuclear pore complex protein Nup155	NUP155
P62244;I3L3P7	4.58E-01	2.43E-01	2.68E-01	1.09E+00	7.51E-03	1.20E-02	40S ribosomal protein S15a	RPS15A
Q495G5;Q8IVH4;D6RIS5	7.06E-01	1.79E-01	2.13E-01	1.94E+00	6.61E-04	1.66E-03	Methylmalonic aciduria type A protein, mitochondrial	MMAA

197

Pneumolysin is responsible for changes in the relative abundance of histone post-translational modifications:

Having defined a pneumolysin-dependent alteration of the macrophage transcriptome and proteome in response to *S. pneumoniae*, we sought next to establish if PLY also influenced epigenetic changes in response to *S. pneumoniae*. Quantitative mass spectrometry was used to identify changes in the global abundance of histone PTMs following challenge with *S. pneumoniae* or ΔPLY. Focussing on the most abundant PTMs, methylation and acetylation, on histones H3 and H4, in MDMs in response to bacterial challenge we identified 94 different peptide proteoforms and 18 were found to change in response to bacterial challenge (Fig 3 & 4). A subset of these changes were PLY-dependent, since they were significantly altered in *S. pneumoniae* in comparison to the ΔPLY mutant (Table 2). These included significant increases in the relative abundance of H3K4me1 and H3.3K36me2 following challenge with *S. pneumoniae* in comparison to ΔPLY. In addition, we observed decreases in the relative abundance of H3K9me2, H3K27me2 and H3K79me2 in a pneumolysin-dependent manner compared to both mock infected (MI; blue) and ΔPLY (Fig 3). Moreover, there was a pneumococcal associated PLY-independent increase in the level of H3K27me2K36me2 and a reciprocal drop in H3K27me3K36me1. We noted an increase in the relative abundance of H3.3K36me2 in a PLY dependent manner and an increase in the relative abundance of H3K23ac and an increase in H3.3K27me2K36me1 with a reciprocal drop in H3.3K27me2K36me2 in response to both bacterial challenges.

222   Table 2: Summary of the significant changes in relative abundance of histone PTMs

223   identified following bacterial challenge

Histone PTM	*S. pneumoniae*	ΔPLY
H3K4me1	Up	Down
H3K9me2	Down	Up
H3K23ac	Up	Up
H3K27me2	Down	Up
H3K27me2K36me2		Up
H3K27me3K36me1		Down
H3.3K27me2K36me1	Up	Up
H3.3K27me2K36me2	Down	Down
H3.3K36me2	Up	Down
H3K79me2	Down	Up

224

225   Further analysis of histone H4 showed a significant increase in the

226   abundance of acetylation on K16 (H4K16ac) in response to infection with either strain

227   (Fig 4). In addition, there was also a decrease in the dimethylated form of K20

228   (H4K20me2) and a reciprocal increase in the monomethylated form (H4K20me1) in a

229   pneumolysin-dependent manner.

230   **Pneumolysin blunts inflammatory signalling during early infection:**

231   In order to establish the consequences of these changes to the transcriptome

232   and epigenome, we next selected one prominent immune signature regulated by

233   pneumolysin, TNF-α expression, and established this as a key component of the early

234   immune response to *S. pneumoniae* (Jones et al. 2005). Using qRT-PCR we

235   measured the abundance of TNFα mRNA in infected MDMs. There was a significant

236   increase in the TNFα mRNA level following infection with the PLY deficient mutant but

237   not the parent strain or the reconstituted mutant (Fig 5A). Next, we measured the

238   amount of secreted of TNFα in MDM supernatants following 3 h of bacterial challenge

239 (Fig 5B). We found that TNFα levels were significantly higher following challenge with

240 the ΔPLY mutant suggesting that PLY initially blunts TNF-α expression.

241   Finally, we measured the concentration of TNFα over time using ELISA

242 assays to determine if this initial anti-inflammatory effect was maintained (Fig 5C). The

243 results showed that the difference seen in the release of TNF-α, was only observed at

244 an early time window, 3-5 h after exposure to bacteria. This suggests that the anti-

245 inflammatory effect of pneumolysin only plays a role over a defined time period.

246

247 **Histone deacetylase inhibitors reduce TNFα cytokines in response to infection:**

248   Having previously demonstrated that pneumolysin both modifies

249 macrophage transcriptome and epigenome we next tested if epigenetic modifications

250 could alter key PLY-associated immune responses. As a proof of concept, we pre-

251 treated MDMs with the histone deacetylase inhibitor (HDACi) vorinostat (SAHA) or

252 vehicle control (DMSO) following challenge with *Streptococcus pneumoniae* or ΔPLY

253 mutant and quantified TNFα release (Fig 6). As previously shown, challenge with the

254 ΔPLY mutant strain resulted in significantly increased TNFα levels as compared to the

255 parental strain, but this level was significantly decreased in the ΔPLY mutant

256 challenged cells by pre-treatment with vorinostat. This suggests that the epigenetic

257 modifications we observed as being induced by PLY exposure could have functional

258 consequences to immune responses, as illustrated for TNFα.

259

260 **Discussion:**

261   Using a range of systems level approaches we have demonstrated that

262 pneumolysin exerts a strong influence over the host response to *S. pneumoniae* at the

263 transcriptomic, proteomic and epigenetic level. We have shown that 503 probes were

14

264 differentially expressed in pneumolysin-dependent manner in association with global

265 pneumolysin dependent changes in histone PTMs. These changes are associated

266 with widespread changes in macrophage metabolism, oxidative stress responses and

267 cytokine signalling and result in differential expression of key immune proteins,

268 including TNF-α and IL-6. Crucially we show that use of a HDAC inhibitor to modify

269 the epigenome is sufficient to reprise the reduction in TNF-α identified as occurring in

270 response to pneumolysin.

271   Our results on the transcriptional response of macrophages to pneumolysin are

272 consistent with previous transcriptomic analysis in undifferentiated THP-1 cells that

273 showed 142 genes to be differentially expressed in a PLY dependent manner and 40

274 to be PLY independent (Rogers et al. 2003). Our study in primary cells, identifies many

275 more genes differentially regulated enabling more in-depth analysis of changes at a

276 pathway level. A number of differentially expressed genes are involved in the immune

277 response such as TNF and HMOX1. Pathway analysis of the differentially expressed

278 probes highlighted the importance of metabolic pathways in response to infection, and

279 in particular the role for oxidative stress responses. The host's oxidative stress

280 responses have been highlighted as playing a key role in the host response to *S*

281 *pneumoniae* in lung epithelial cells (Zahlten et al. 2015). Importantly, this module is

282 upregulated in alveolar macrophages (AM) and plays a key role in preserving

283 responses such as phagocytosis which may otherwise be altered by dysregulated

284 oxidative stress in AM and MDM (Bewley et al. 2014; Belchamber et al. 2019).

285 Furthermore, nuclear factor erythroid 2 (NRF2), the master regulator of antioxidant

286 responses, plays a pivotal role in the protection against lung injury (Zhao et al. 2017),

287 reduces lung inflammation after intratracheal instillation of LPS and decreases

288 mortality in systemic models of inflammation (Thimmulappa et al., 2016). Crucially,

289   NRF2-regulated pathways are amenable to therapeutic manipulation as evidenced by

290   improved AM phagocytosis in patients with chronic obstructive pulmonary disease

291   following *ex vivo* treatment with NRF2 agonists and also in a mouse model of cigarette

292   smoke associated impairment of bacterial clearance in the lung (Harvey et al. 2011).

293   The XGR pathway analysis following bacterial challenge further highlighted NFkB,

294   NOD-like receptor and TNF signalling as enriched pathways emphasising their

295   importance in the host's response to bacteria.

296   The label-free quantitative proteomic analysis revealed a small number of

297   significantly differentially expressed proteins, but substantiated involvement of several

298   of the pathways identified at the transcriptomic pathway level. Examples of proteins

299   linked to these pathways included an increase in the coiled-coil domain containing

300   protein 22 (CCDC22), that plays an essential role in NFKB signalling and whose

301   depletion leads to blockade of signalling (Starokadomskyy et al. 2013). As an example

302   of a protein downregulated we noted that the oxidative stress response protein 1

303   (OXSR1) involved in the oxidative stress response (W. Chen, Yazicioglu, and Cobb

304   2004) was decreased in a PLY-dependent manner.

305   The proteomic analysis also identified a number of differentially expressed

306   proteins that are involved in regulating gene transcription and protein translation. The

307   probable global transcription activator SNF2L2 / Brahma and the transcription

308   activator Brahma-related gene 1 proteins were decreased in PLY dependent manner.

309   They are associated with regulation of gene transcription by chromatin remodelling (B.

310   G. Wilson and Roberts 2011). The ATP dependent RNA helicase DDX46 which is

311   associated with pre-mRNA splicing (Will et al. 2002) was also increased in a PLY

312   dependent manner. In addition, we observed an increase in the probable 28S rRNA

313   (cytosine(4447)-C(5))-methyltransferase encoded for by the NOP2 gene which has

314   been shown to be associated with the assembly of the large subunit of the ribosome

315   and may play a role in cell cycle and proliferation (Sloan, Bohnsack, and Watkins

316   2013). In summary, the quantitative proteomic analysis identified a number of

317   pneumolysin-dependent differentially expressed proteins involved in the regulation of

318   gene transcription, protein translation, and modulation of signalling pathways such as

319   the NFkB pathway, which are predicted to regulate innate immune responses to

320   bacteria.

321   Although the absolute number of differentially expressed proteins is small, these

322   results are in keeping with a number of previously published proteomic studies. In a

323   study of THP-1 cells infected with *Mycobaterium tuberculosis* only 61 proteins were

324   found to be differentially regulated (P. Li et al. 2017). In a study of alveolar

325   macrophages infected with porcine reproductive and respiratory syndrome virus only

326   95 proteins were differentially expressed (Qu et al. 2017). Furthermore, this study has

327   used primary cells and one of the reasons for the relatively small number of

328   differentially expressed proteins may be the large differences between the biological

329   replicates such that small differences in protein abundances following infection may

330   not reach statistical significance. Several studies have shown only modest correlation

331   between transcriptomic and proteomic datasets (Stare et al. 2017; G. Chen et al. 2002;

332   Pascal et al. 2008; Ghazalpour et al. 2011), which might further explain the small

333   number of differentially expressed proteins. Moreover, the transition from altered

334   transcriptional response to altered proteome may take longer than the 6 hour time

335   point studied. Indeed, in the study of proteomic response to *M. tuberculosis* and

336   pathogenic porcine reproductive and respiratory syndrome virus both authors used a

337   24 hour time point (H. Li et al. 2017; Qu et al. 2017). It is also possible that many of

17

338   the differentially expressed proteins are of relatively low abundance and therefore not

339   readily detected using a shotgun proteomics approach.

340   Finally, the quantitative mass spectrometry analysis of histone PTMs in response

341   to *S pneumoniae* was used to identify and quantify 94 different peptide proteoforms.

342   Of these, there were 5 whose relative abundance changed in a pneumolysin

343   dependent manner. This is to our knowledge the first time that this approach has been

344   applied to study the changes in relative abundance of histone PTMs in primary MDMs

345   in response to *S. pneumoniae.* The advantages of mass spectrometry analysis used

346   in this study were emphasised by the identification of combinatorial marks on both H3

347   and H3.3 that would not have been possible using antibody-based approaches.

348   Interestingly several of these modifications are associated with activating or

349   repressing gene transcription. Although some histone PTMs are well characterised in

350   a number of systems, their exact function in the context of infections is yet to be fully

351   described. It is likely to vary between cell types. Furthermore, individual PTMs will not

352   act in isolation but rather be part of a combinatorial code fine tuning responses to

353   environmental stressors, such as to bacterial infection and at later time points after

354   exposure to consequences such as DNA damage. Nevertheless, in light of the

355   changes observed in response to challenge with *S. pneumoniae* (*e.g.* increases in

356   H3K4me1, H3K23ac or H4K16ac and decreases in H3K9me2 or H3K79me2) it is

357   possible that these changes represent the removal of repressive marks and the

358   increase in marks associated with active gene transcription. This would allow fine

359   tuning of the innate immune host response to bacteria to occur. This highlights the

360   important role played by PTMs in the response to infection and therefore offer the

361   potential for the novel use of therapeutic approaches involving immunomodulation of

362   host responses through the use of emerging classes of drugs that target the enzymes

363   that regulate these histone PTMs.

364   The functional consequences of the net changes to transcriptional responses

365   involving inflammatory cell signalling and regulation of protein expression were

366   examined focusing on TNF-α as an exemplar early response cytokine that plays a key

367   role against *S. pneumoniae* (Jones et al. 2005). We selected this cytokine since PLY

368   induced a significant temporal reduction in production of TNF-α, in conjunction with

369   decreased production of IL-6. Our demonstration that pneumolysin inhibits the early

370   production of TNF-α is consistent with the findings others have reported in dendritic

371   cells and murine AM (Subramanian et al. 2019). We were able to demonstrate that

372   changes in the epigenetic landscape are sufficient to reverse the maximal induction of

373   TNF-α production observed following challenge with the PLY-deficient mutant. These

374   experiments, using a HDACi, suggest that blunting of TNF-α release by MDM following

375   challenge with a pneumococcal strain expressing PLY could be mediated through

376   epigenetic mechanisms. This is important since early response cytokine generation is

377   critical to the outcome of infection in *S. pneumoniae* and any modulation through

378   reshaping the epigenetic landscape would be anticipated to have major consequences

379   to the outcome of infection. Of note, the HDAC inhibitor Cambinol has been shown to

380   inhibit TNF and IL-6 secretion in bone marrow-derived macrophages stimulated with

381   LPS and was associated with greater survival in a murine lethal endotoxemia model

382   and in response to *Klebsiella pneumoniae* challenge (Lugrin et al. 2013). In this case

383   the therapeutic intervention was thought to limit excessive cytokine responses

384   whereas in the case of PLY we would suggest it may limit early cytokine responses

385   required to enhance early pathogen control. This emphasizes that in line with other

386   aspects of host modulation through epigenetic manipulation would require careful

387   calibration.

388

389   In summary our findings using a range of systems levels approaches show that

390   pneumolysin modifies the early host response of macrophages to *S. pneumoniae*

391   through modification of inflammatory responses, resistance to oxidative stress and

392   metabolic responses. We observe that these transcriptional responses and the

393   differential protein expression are associated with global changes in histone PTMs.

394   We show alteration of the epigenetic landscape has functional consequences to key

395   immune responses such as TNF-α production and suggest that PLY exerts these

396   affects through epigenetic modulation and regulation of histone acetylation status. Our

397   results also hint at a potential route by which these early host responses can be altered

398   to improve responses to infection through the use of agents that modulate the

399   enzymes that induce the signature pathogen-mediated epigenetic marks that

400   adversely impact host responses.

401

402

Materials and methods:

Bacterial Strains:

Streptococcus pneumoniae serotype 2 strain D39 (D39), the isogenic pneumolysin-deficient mutant D39-ΔPLY (ΔPLY), which has a single amino acid substitution in the pneumolysin sequence generating a STOP codon and the reconstituted mutant PLY-D39-ΔPLY, which expresses PLY under an erythromycin promoter, were kindly obtained from Prof T. Mitchell (University of Birmingham). These were cultured and characterized as previously described (Bewley et al. 2014). Strains were grown in brain heart infusion broth and 20% FCS to mid exponential phase (with or without 1μg/mL erythromycin).

MDM infection:

Whole blood was obtained from healthy volunteers. Ethical approval was granted by South Sheffield Regional Ethics committee (07/Q2305/7). Peripheral blood mononuclear cells were separated by differential centrifugation using a Ficoll-Paque gradient and differentiated into monocyte derived macrophages (MDM) for 14 d as previously described in 24 well plates (Corning) (Collini et al. 2018). Bacteria were washed in PBS and re-suspended in RPMI 1640 supplemented with 10% pooled human immune serum (from previously vaccinated volunteers with demonstrable antibody levels to serotype 2 pneumococci) (Gordon et al. 2000). MDM were challenged with either opsonised D39, ΔPLY or PBS, at a MOI of 10, rested on ice for 1 h and incubated at 37°C in 5% CO_2 for a further 3 h (Minshull et al. 2016). For certain experiments cells were treated with 3 μM vorinostat (SAHA, Sigma) or 0.5% DMSO (vehicle control) for 30 min prior to bacterial challenge and vorinostat reintroduced after bacterial challenge.

S. pneumoniae **internalisation assay:**

428

429 MDM were challenged with opsonized *S. pneumoniae* for 3 h then washed

430 three times in PBS, incubated for 30 min in RPMI media (Lonza) with 40 units/mL of

431 benzylpenicillin (Sigma) and 20 mg/mL gentamicin (Sanofi). The cells were then

432 washed three times in PBS and incubated in 250 μL of 2% saponin (Sigma) for 12 min

433 at 37°C in 5% CO_2, then 750 μL of PBS was added, followed by vigorous pipetting.

434 The number of internalised viable bacteria were measured by counting the number of

435 colony forming units on Colombia blood agar (CBA) after 24 h incubation at 37°C in

436 5% CO_2 contained in these lysates measured in triplicate.

Cytokine measurements:

437

438 Supernatants were obtained from MDM challenged with bacteria and were

439 analysed as per the manufacturers protocol using either Tumour necrosis factor alpha

440 (TNF-α (Ready-set-go!™, eBioscience)) or interleukin 6 (IL-6kit (Ready-set-go!™,

441 eBioscience)). Briefly, 96 well ELISA plates were coated with 100 μL of 1x capture

442 antibody overnight at 4°C, washed, and blocked in 200 μL assay diluent for 1 h at

443 room temperature. After a wash, the supernatants were then added as were the

444 standards (recombinant human TNF-α or recombinant human IL-6) and incubated for

445 2 h at room temperature. The wells were then washed and the detection antibody

446 (biotin-conjugated anti-human TNF-α or anti-human IL-6) was added. After washing

447 100 μL avidin-horse radish peroxidase (HRP) was added to each well for 30 min at

448 room temperature. Plates were then washed, prior to adding 100uL

449 tetramethylbenzidine substrate solution for 15 at room temperature. The reaction was

450 stopped by adding 2M sulphuric acid, the plate was then read at 450 nm using a

451 Multiskan® EX plate reader (Thermo Scientific), and the data analysed in GraphPad

452 Prism version 7.0c. (GraphPad Software).

22

RNA Extraction:

453

454   After 3 h of bacterial challenge, cells were washed and lysed in 600 µL Tri

455 Reagent (Sigma) for 15min at room temperature before storing at -80 C. Ribonucleic

456 acid (RNA) extraction was performed following the manufacturers guidelines for

457 Direct-Zol™ RNA miniPrep (Zymo). Briefly, samples in Tri Reagent® were centrifuged

458 at 12 000g for 1 min, then the supernatant was transferred to a fresh 1.5 mL tube,

459 100% ethanol was added in a 1:1 ratio and well mixed. This was then transferred to

460 the Zymo-spin™ column, centrifuged for 1 min, then washed using 400 µL Direct-Zol™

461 RNA pre-wash, centrifuged again at 12 000g for 1 min, then washed in 700 µL RNA

462 wash buffer and again centrifuged at 12 000g for 1 min. Finally the RNA was eluted

463 out in 50µl DNase/RNase free water.

Microarray mRNA expression analysis:

464

465   Affymetrix chip micro-array (Human Genome U133 plus 2.0 array, Santa Clara,

466 CA) analysis of samples from three individuals was undertaken to characterise gene

467 expression as previously described(Bewley et al. 2018). Data analysis was performed

468 as previously described (Bewley et al. 2018). Briefly, CEL files were analysed using R

469 version 3.4.0 . CEL files were read using *Simpleaffy* version 2.52.0(C. L. Wilson and

470 Miller 2005); background intensity correction, median correction and quantile probeset

471 normalisation was performed using robust multi-array average expression with the

472 help of probe sequence (GCRMA), using *AffyPLM* version 1.52.1(Bolstad et al. 2005).

473 The quality control matrix was generated using *Simpleaffy* and *AffyPLM*. Principal

474 component analysis was performed in R. The probes whose intensity were within the

475 lowest 20th centile were removed, using Dplyr version 0.7.1. Differential gene

476 expression was calculated using *Limma* version 3.32.2.

23

477 **Pathway analysis:**

478 Pathway analysis was performed from the differentially-expressed gene lists

479 generated. Hypergeometric tests were calculated in R, using *GO.db* version 3.4.1 to

480 search the Gene Ontology (GO) database (Ashburner et al. 2000)for molecular

481 function, cellular component, and biological process, using a p value cut off of 0.01

482 and a minimum of 3 genes. In addition, canonical pathway analysis was performed

483 using XGR (1.1.5) (H. Fang et al. 2016) using all of the differentially expressed probes

484 identified by ANOVA calculated in *Limma* as the test background.

485

486 **Real time quantitative polymerase chain reaction (RT-PCR):**

487 The abundance of TNFα mRNA in bacterial exposed and mock-infected MDM was

488 measured using qPCR. To perform cDNA synthesis a high-capacity cDNA reverse

489 transcription kit (Applied Biosystems) was used to make complementary DNA for

490 qPCR assay as per manufacturers protocol. The DNA products were quantified on

491 QuantStudio5 (Abi) using GoTaq qPCR master mix (Promega). The reactions were

492 prepared as per manufacturers protocol.

493 Primers used:

494 TNFα: Forward 5' CTCTTCTGCCTGCTGCACTTG 3'

495 Reverse 5' ATGGGCTACAGGCTTGTCACTC 3'

496 GAPDH: Forward 5' TGCACCACCAACTGCTTAGC 3'

497 Reverse 5' GGCATGGACTGTGGTCATGAG 3'

498 Actin: Forward 5' CCTTTGCCGATCCGCCG 3'

499 Reverse 5' GATATCATCATCCATGGTGAGCTGG 3'

500 Fold change was calculated using Delta Delta Ct values.

501

24

502 **Quantitative proteomics:**

503 Protein lysates were digested with trypsin in conjunction with the Filter aided

504 separation protocol (FASP) (Wiśniewski et al. 2009). Briefly, cells were lysed in 150

505 µL of 4% Sodium dodecyl sulphate (Sigma), 100 mM Tris HCl (Sigma) pH 7.6, 0.1 M

506 Dithiothreitol (Sigma) and quantified using a BioRad DC assay as per the

507 manufacturers protocol. 100 µg of protein lysates were mixed with 200 µL of 8 M

508 urea dissolved in triethylammonium bicarbonate (TEAB) and added to the filter

509 mounted in 11.5 mL low-bind Eppendorf. The tubes were centrifuged at 14 000 g for

510 30 min, the flow through discarded and further two 200 µL washes in 8M urea were

511 performed. Then 100 µL 0.5 M iodoacetic acid was added for 20 min at room

512 temperature and then centrifuged at 14 000 g for 30 min. The flow-through was

513 discarded. The membrane was washed three times with 100 µL of 8 M urea,

514 followed by three washes 100 mM TEAB. The lysates were trypsin digested

515 overnight at 37 °C. The digested proteins were eluted in 120 µL 100mM TEAB. The

516 samples were then desalted using Hypersep Hypercarb^{TM} (ThermoScientific) tips

517 following the manufacturers protocol. Briefly, tips were primed with elution solution

518 (60% Acetonitrile 0.1% TFA) then washed in 0.1% TFA. The sample was then re-

519 suspended on the tip by pipetting up and down 50 times. The tip was cleaned in

520 0.1%TFA, eluted 60% ACN 0.1% TFA and then 90% ACN 0.1% TFA. The samples

521 were then dried down in Speedvac (Eppendorf). The peptides were re-suspended in

522 0.1%TFA and 3% ACN and loaded into and run on Ultimate 3000 RSLC nano flow

523 liquid chromatography system with a PepMap300 C18 trapping column (Thermo

524 Fisher), coupled to Q-Exactive HF Orbitrap mass spectrometer (Thermo Fisher).

525 Peptides were eluted onto a 50 cm x 75 µm Easy-spray PepMap C18 column with a

526 flow rate of 300 nL/min as previously described (Cole et al. 2019). Peptides were

527   eluted using a gradient of 3% to 35% solvent B over 75 min. Solvents were

528   composed of 0.1% formic acid (FA) and either 3% acetonitrile (ACN) (Solvent A) or

529   80% ACN (Solvent B). The loading solvent was 0.1% TFA and 3% ACN. Data

530   acquisition was performed in full scan positive mode, scanning 375 to 1500m/z, with

531   an MS1 resolution of 120 000, and AGC target of $1x10^6$. The top 10 most intense

532   ions from MS1 scan were selected for Collision induced dissociation. MS2 resolution

533   was of 30 000 with AGC target of $1x10^5$ and maximum fill time of 60 ms, with an

534   isolation window of 2 m/z and scan range of 200-2000 m/z and normalised collision

535   energy of 27.

MaxQuant data analysis:

537   The raw data from the MS were analysed in MaxQuant (version 1.5.6.5). The

538   database search engine Andromeda was used to search the spectra against the

539   UniProt database. The search settings were as follows: trypsin/P digestion, with up to

540   2 miss.ed cleavages, fixed modification was carbamidomethyl (C), variable

541   modifications were oxidation (M) and acetylation (Protein N-term), Label Free

542   Quantification (LFQ) was performed with a minimum number of neighbours of 3 and

543   average number of neighbour of 6. Peptide tolerance was set at 4.5 ppm and minimum

544   peptide length was set at 7, amino acid maximum peptide mass was set at of 4600 Da

545   and Protein FDR was set at 0.01. Downstream analysis was performed in R version

546   3.4.0. The protein identification files were read in, results matching to a reverse

547   sequence database and or those matching to a contaminant database were removed

548   as were those with less than 2 unique peptides. The label-free intensities were then

549   median-corrected for each sample and log2 transformed. Differential protein

550   expression was calculated using Limma version 3.32.2. a repeated measures ANOVA

551   to enable comparison to the microarray analysis (Goeminne, Gevaert, and Clement

552   2016).

Histone extraction:

554   Histone extraction was performed as previously described (Shechter et al.

555   2007). Briefly, MDMs were washed in PBS and scrapped in ice cold PBS with 1x

556   protease inhibitors (Roche Complete EDTA free), before being pelleted at 900g for 10

557   min. Cell pellets were lysed in hypotonic lysis solution then re-suspended in 400 µL

558   0.2 M H_2SO_4. The histones were precipitated out by adding 132uL of 6.1N TCA to the

559   supernatant and washed in acetone then resuspended in 100 µL of water (HPLC

560   grade). Samples then underwent chemical derivitisation as previously described

561   (Garcia et al. 2007). 10 µL of 100 mM ammonium bicarbonate pH 8 and 4 µl of

562   ammonium hydroxide was added to 10 µg of histone sample. Then 10 µL of propionic

563   anhydride in isopropanol (1:3 ratio) was added and 100% ammonium hydroxide used

564   to keep the pH >8.0. The sample was incubated at 37°C for 15 min. Then it was dried

565   down in a vacuum centrifuge (Concentrator plus, Eppendorf) and the process

566   repeated. The samples were re-suspended in 40 µL of 100 mM ammonium

567   bicarbonate and then tryptically digested overnight. The digestion was stopped by

568   addition of glacial acetic acid and freezing at -80°C for 5 min. Finally, the samples

569   were dried down before undergoing a further two rounds of proprionylation.

570   Hypersep™ Hypercarb™ tip were used to desalt the samples of the chemical

571   derivitisation residues following the manufacturers protocol for Hypersep ™ Hypercarb

572   ™ (ThermoScientific). (Minshull et al. 2016).

Quantitative MS analysis of histone PTMs

574   The histone samples were re-suspended in 0.1% trifluoroacetic acid (TFA) and

575   were analyzed on an Ultimate 3000 online nano-LC system with a PepMap300 C18

27

576 trapping column (ThermoFisher Scientific), coupled to a Q Exactive HF Orbitrap

577 (ThermoFisher Scientific). Peptides were eluted onto a 50 cm × 75 µm Easy-spray

578 PepMap C18 analytical column at 35°C. Peptides were eluted at a flow rate of

579 300 nL/min using a gradient of 3% to 25% over 55 min then 25% to 60% until 81 min.

580 Solvents were composed of 0.1% formic acid (FA) and either 3% acetonitrile (ACN)

581 (solvent A) or 80% ACN (solvent B). The loading solvent was 0.1% TFA and 3% ACN

582 run in Data independent acquisition as previously described (Cole et al. 2019). The

583 PTM identification and relative abundance was performed in Skyline and Epiprofile 2.0

584 also as previously described (Cole et al. 2019).

585 **Statistical analysis:**

586 Statistical analysis was performed using either R for the microarray and

587 proteomic analysis, or for all other experiments in Prism version 7.0c (Graphpad). Data

588 is presented as standard deviation (SD) or standard error of the mean (SEM). For all

589 experiments a minimum of 3 biological replicates was used. Comparison between two

590 paired groups employed a paired t-test, for comparison of 3 or more conditions a one-

591 way analysis of variance (ANOVA) with Tukey's post-test was performed. For

592 comparison of multiple observations in more than two groups a two-way ANOVA with

593 Tukey's multiple comparison post-test was performed.

594

References:

Ashburner, Michael, Catherine A. Ball, Judith A. Blake, David Botstein, Heather Butler, J. Michael Cherry, Allan P. Davis, et al. 2000. "Gene Ontology: Tool for the Unification of Biology." *Nature Genetics* 25 (1): 25–29. https://doi.org/10.1038/75556.

Belchamber, Kylie B. R., Richa Singh, Craig M. Batista, Moira K. Whyte, David H. Dockrell, Iain Kilty, Matthew J. Robinson, Jadwiga A. Wedzicha, Peter J. Barnes, and Louise E. Donnelly. 2019. "Defective Bacterial Phagocytosis Is Associated with Dysfunctional Mitochondria in COPD Macrophages." *European Respiratory Journal*, January. https://doi.org/10.1183/13993003.02244-2018.

Benton, K A, M P Everson, and D E Briles. 1995. "A Pneumolysin-Negative Mutant of Streptococcus Pneumoniae Causes Chronic Bacteremia Rather than Acute Sepsis in Mice." *Infection and Immunity* 63 (2): 448–55.

Berger, Shelley L. 2007. "The Complex Language of Chromatin Regulation during Transcription." *Nature* 447 (7143): 407–12. https://doi.org/10.1038/nature05915.

Bewley, Martin A., Richard C. Budd, Eilise Ryan, Joby Cole, Paul Collini, Jennifer Marshall, Umme Kolsum, et al. 2018. "Opsonic Phagocytosis in Chronic Obstructive Pulmonary Disease Is Enhanced by Nrf2 Agonists." *American Journal of Respiratory and Critical Care Medicine* 198 (6): 739–50. https://doi.org/10.1164/rccm.201705-0903OC.

Bewley, Martin A., Michael Naughton, Julie Preston, Andrea Mitchell, Ashleigh Holmes, Helen M. Marriott, Robert C. Read, Timothy J. Mitchell, Moira K. B. Whyte, and David H. Dockrell. 2014. "Pneumolysin Activates Macrophage Lysosomal Membrane Permeabilization and Executes Apoptosis by Distinct Mechanisms without Membrane Pore Formation." *MBio* 5 (5). https://doi.org/10.1128/mBio.01710-14.

Bolstad, B. M., F. Collin, J. Brettschneider, K. Simpson, L. Cope, R. A. Irizarry, and T.P. Speed. 2005. "Quality Assessment of Affymetrix GeneChip Data." In *Bioinformatics and Computational Biology Solutions Using R and Bioconductor*, edited by Robert Gentleman, Vincent J. Carey, Wolfgang Huber, Rafael A. Irizarry, and Sandrine Dudoit, 33–47. Statistics for Biology and Health. New York, NY: Springer. https://doi.org/10.1007/0-387-29362-0_3.

Breuilh, Laetitia, François Vanhoutte, Josette Fontaine, Caroline M. W. van Stijn, Isabelle Tillie-Leblond, Monique Capron, Christelle Faveeuw, et al. 2007. "Galectin-3 Modulates Immune and Inflammatory Responses during Helminthic Infection: Impact of Galectin-3 Deficiency on the Functions of Dendritic Cells." *Infection and Immunity* 75 (11): 5148–57. https://doi.org/10.1128/IAI.02006-06.

Chen, Guoan, Tarek G. Gharib, Chiang-Ching Huang, Jeremy M. G. Taylor, David E. Misek, Sharon L. R. Kardia, Thomas J. Giordano, et al. 2002. "Discordant Protein and MRNA Expression in Lung Adenocarcinomas." *Molecular & Cellular Proteomics* 1 (4): 304–13. https://doi.org/10.1074/mcp.M200008-MCP200.

Chen, Wei, Mustafa Yazicioglu, and Melanie H. Cobb. 2004. "Characterization of OSR1, a Member of the Mammalian Ste20p/Germinal Center Kinase

Subfamily." *Journal of Biological Chemistry* 279 (12): 11129–36. https://doi.org/10.1074/jbc.M313562200.

Cole, Joby, Eleanor J. Hanson, David C. James, David H. Dockrell, and Mark J. Dickman. 2019. "Comparison of Data-acquisition Methods for the Identification and Quantification of Histone Post-translational Modifications on a Q Exactive HF Hybrid Quadrupole Orbitrap Mass Spectrometer." *Rapid Communications in Mass Spectrometry* 33 (10): 897–906. https://doi.org/10.1002/rcm.8401.

Cole, Joby, Paul Morris, Mark J. Dickman, and David H. Dockrell. 2016. "The Therapeutic Potential of Epigenetic Manipulation during Infectious Diseases." *Pharmacology & Therapeutics* 167 (November): 85–99. https://doi.org/10.1016/j.pharmthera.2016.07.013.

Collini, Paul J., Martin A. Bewley, Mohamed Mohasin, Helen M. Marriott, Robert F. Miller, Anna-Maria Geretti, Apostolos Beloukas, et al. 2018. "HIV Gp120 in the Lungs of Antiretroviral Therapy–Treated Individuals Impairs Alveolar Macrophage Responses to Pneumococci." *American Journal of Respiratory and Critical Care Medicine* 197 (12): 1604–15. https://doi.org/10.1164/rccm.201708-1755OC.

Eskandarian, Haig A, Francis Impens, Marie-Anne Nahori, Guillaume Soubigou, Jean-Yves Coppée, Pascale Cossart, and Mélanie A Hamon. 2013. "A Role for SIRT2-Dependent Histone H3K18 Deacetylation in Bacterial Infection." *Science (New York, N.Y.)* 341 (6145): 1238858. https://doi.org/10.1126/science.1238858.

Fang, Hai, Bogdan Knezevic, Katie L. Burnham, and Julian C. Knight. 2016. "XGR Software for Enhanced Interpretation of Genomic Summary Data, Illustrated by Application to Immunological Traits." *Genome Medicine* 8 (1): 129. https://doi.org/10.1186/s13073-016-0384-y.

Fang, Rendong, Kohsuke Tsuchiya, Ikuo Kawamura, Yanna Shen, Hideki Hara, Shunsuke Sakai, Takeshi Yamamoto, et al. 2011. "Critical Roles of ASC Inflammasomes in Caspase-1 Activation and Host Innate Resistance to Streptococcus Pneumoniae Infection." *Journal of Immunology (Baltimore, Md.: 1950)* 187 (9): 4890–99. https://doi.org/10.4049/jimmunol.1100381.

Garcia, Benjamin A, Sahana Mollah, Beatrix M Ueberheide, Scott A Busby, Tara L Muratore, Jeffrey Shabanowitz, and Donald F Hunt. 2007. "Chemical Derivatization of Histones for Facilitated Analysis by Mass Spectrometry." *Nature Protocols* 2 (4): 933–38. https://doi.org/10.1038/nprot.2007.106.

Ghazalpour, Anatole, Brian Bennett, Vladislav A. Petyuk, Luz Orozco, Raffi Hagopian, Imran N. Mungrue, Charles R. Farber, et al. 2011. "Comparative Analysis of Proteome and Transcriptome Variation in Mouse." *PLoS Genetics* 7 (6). https://doi.org/10.1371/journal.pgen.1001393.

Goeminne, Ludger J. E., Kris Gevaert, and Lieven Clement. 2016. "Peptide-Level Robust Ridge Regression Improves Estimation, Sensitivity, and Specificity in Data-Dependent Quantitative Label-Free Shotgun Proteomics." *Molecular & Cellular Proteomics* 15 (2): 657–68. https://doi.org/10.1074/mcp.M115.055897.

Gordon, Stephen B., Glen R. B. Irving, Roderick A. Lawson, Margaret E. Lee, and Robert C. Read. 2000. "Intracellular Trafficking and Killing of Streptococcus Pneumoniae by Human Alveolar Macrophages Are Influenced by Opsonins." *Infection and Immunity* 68 (4): 2286–93.

Gray, Barry M., George M. Converse, and Hugh C. Dillon. 1980. "Epidemiologic Studies of Streptococcus Pneumoniae in Infants: Acquisition, Carriage, and Infection during the First 24 Months of Life." *The Journal of Infectious Diseases* 142 (6): 923–33. https://doi.org/10.1093/infdis/142.6.923.

Hamon, Mélanie Anne, Eric Batsché, Béatrice Régnault, To Nam Tham, Stéphanie Seveau, Christian Muchardt, and Pascale Cossart. 2007. "Histone Modifications Induced by a Family of Bacterial Toxins." *Proceedings of the National Academy of Sciences of the United States of America* 104 (33): 13467–72. https://doi.org/10.1073/pnas.0702729104.

Harvey, Christopher J., Rajesh K. Thimmulappa, Sanjay Sethi, Xiaoni Kong, Lonny Yarmus, Robert H. Brown, David Feller-Kopman, Robert Wise, and Shyam Biswal. 2011. "Targeting Nrf2 Signaling Improves Bacterial Clearance by Alveolar Macrophages in Patients with COPD and in a Mouse Model." *Science Translational Medicine* 3 (78): 78ra32-78ra32. https://doi.org/10.1126/scitranslmed.3002042.

Houldsworth, S, P W Andrew, and T J Mitchell. 1994. "Pneumolysin Stimulates Production of Tumor Necrosis Factor Alpha and Interleukin-1 Beta by Human Mononuclear Phagocytes." *Infection and Immunity* 62 (4): 1501–3.

Hu, Da-Kang, Yang Liu, Xiang-Yang Li, and Ying Qu. 2015. "In Vitro Expression of Streptococcus Pneumoniae Ply Gene in Human Monocytes and Pneumocytes." *European Journal of Medical Research* 20 (1). https://doi.org/10.1186/s40001-015-0142-4.

Hu, Hongbo, and Shao-Cong Sun. 2016. "Ubiquitin Signaling in Immune Responses." *Cell Research* 26 (4): 457–83. https://doi.org/10.1038/cr.2016.40.

Jenuwein, T, and C D Allis. 2001. "Translating the Histone Code." *Science (New York, N.Y.)* 293 (5532): 1074–80. https://doi.org/10.1126/science.1063127.

Jones, Matthew R., Benjamin T. Simms, Michal M. Lupa, Mariya S. Kogan, and Joseph P. Mizgerd. 2005. "Lung NF-KB Activation and Neutrophil Recruitment Require IL-1 and TNF Receptor Signaling during Pneumococcal Pneumonia." *The Journal of Immunology* 175 (11): 7530–35. https://doi.org/10.4049/jimmunol.175.11.7530.

Kadioglu, Aras, Jeffrey N. Weiser, James C. Paton, and Peter W. Andrew. 2008. "The Role of Streptococcus Pneumoniae Virulence Factors in Host Respiratory Colonization and Disease." *Nature Reviews Microbiology* 6 (4): 288–301. https://doi.org/10.1038/nrmicro1871.

Li, Hua, Sha Wei, Yuan Fang, Min Li, Xia Li, Zhe Li, Jibin Zhang, et al. 2017. "Quantitative Proteomic Analysis of Host Responses Triggered by Mycobacterium Tuberculosis Infection in Human Macrophage Cells." *Acta Biochimica Et Biophysica Sinica* 49 (9): 835–44. https://doi.org/10.1093/abbs/gmx080.

Li, Pei, Rui Wang, Wenqi Dong, Linlin Hu, Bingbing Zong, Yanyan Zhang, Xiangru Wang, et al. 2017. "Comparative Proteomics Analysis of Human Macrophages Infected with Virulent Mycobacterium Bovis." *Frontiers in Cellular and Infection Microbiology* 7 (March). https://doi.org/10.3389/fcimb.2017.00065.

Lugrin, Jérôme, Eleonora Ciarlo, Alba Santos, Gaël Grandmaison, Isis dos Santos, Didier Le Roy, and Thierry Roger. 2013. "The Sirtuin Inhibitor Cambinol Impairs MAPK Signaling, Inhibits Inflammatory and Innate Immune

Responses and Protects from Septic Shock." *Biochimica Et Biophysica Acta* 1833 (6): 1498–1510. https://doi.org/10.1016/j.bbamcr.2013.03.004.

"Lung NF-KB Activation and Neutrophil Recruitment Require IL-1 and TNF Receptor Signaling during Pneumococcal Pneumonia | The Journal of Immunology." n.d. Accessed April 1, 2020. https://www.jimmunol.org/content/175/11/7530.long.

McNeela, Edel A., Áine Burke, Daniel R. Neill, Cathy Baxter, Vitor E. Fernandes, Daniela Ferreira, Sarah Smeaton, et al. 2010. "Pneumolysin Activates the NLRP3 Inflammasome and Promotes Proinflammatory Cytokines Independently of TLR4." *PLoS Pathog* 6 (11): e1001191. https://doi.org/10.1371/journal.ppat.1001191.

Minshull, Thomas C., Joby Cole, David H. Dockrell, Robert C. Read, and Mark J. Dickman. 2016. "Analysis of Histone Post Translational Modifications in Primary Monocyte Derived Macrophages Using Reverse Phase×reverse Phase Chromatography in Conjunction with Porous Graphitic Carbon Stationary Phase." *Journal of Chromatography. A* 1453 (July): 43–53. https://doi.org/10.1016/j.chroma.2016.05.025.

Pascal, Laura E, Lawrence D True, David S Campbell, Eric W Deutsch, Michael Risk, Ilsa M Coleman, Lillian J Eichner, Peter S Nelson, and Alvin Y Liu. 2008. "Correlation of MRNA and Protein Levels: Cell Type-Specific Gene Expression of Cluster Designation Antigens in the Prostate." *BMC Genomics* 9 (May): 246. https://doi.org/10.1186/1471-2164-9-246.

Paton, J. C., B. Rowan-Kelly, and A. Ferrante. 1984. "Activation of Human Complement by the Pneumococcal Toxin Pneumolysin." *Infection and Immunity* 43 (3): 1085–87.

Pee, Katharina van, Alexander Neuhaus, Edoardo D'Imprima, Deryck J Mills, Werner Kühlbrandt, and Özkan Yildiz. 2017. "CryoEM Structures of Membrane Pore and Prepore Complex Reveal Cytolytic Mechanism of Pneumolysin." Edited by Sjors HW Scheres. *ELife* 6 (March): e23644. https://doi.org/10.7554/eLife.23644.

Qu, Zehui, Fei Gao, Liwei Li, Yujiao Zhang, Yifeng Jiang, Lingxue Yu, Yanjun Zhou, et al. 2017. "Label-Free Quantitative Proteomic Analysis of Differentially Expressed Membrane Proteins of Pulmonary Alveolar Macrophages Infected with Highly Pathogenic Porcine Reproductive and Respiratory Syndrome Virus and Its Attenuated Strain." *Proteomics* 17 (23–24). https://doi.org/10.1002/pmic.201700101.

Quin, Lisa R., Quincy C. Moore, and Larry S. McDaniel. 2007. "Pneumolysin, PspA, and PspC Contribute to Pneumococcal Evasion of Early Innate Immune Responses during Bacteremia in Mice." *Infection and Immunity* 75 (4): 2067–70. https://doi.org/10.1128/IAI.01727-06.

Rogers, P. David, Justin Thornton, Katherine S. Barker, D. Olga McDaniel, Gordon S. Sacks, Edwin Swiatlo, and Larry S. McDaniel. 2003. "Pneumolysin-Dependent and -Independent Gene Expression Identified by CDNA Microarray Analysis of THP-1 Human Mononuclear Cells Stimulated by Streptococcus Pneumoniae." *Infection and Immunity* 71 (4): 2087–94. https://doi.org/10.1128/IAI.71.4.2087-2094.2003.

Rolando, Monica, Serena Sanulli, Christophe Rusniok, Laura Gomez-Valero, Clement Bertholet, Tobias Sahr, Raphael Margueron, and Carmen Buchrieser. 2013. "Legionella Pneumophila Effector RomA Uniquely Modifies Host Chromatin to Repress Gene Expression and Promote Intracellular

Bacterial Replication." *Cell Host & Microbe* 13 (4): 395–405. https://doi.org/10.1016/j.chom.2013.03.004.

Sander, Leif E., Michael J. Davis, Mark V. Boekschoten, Derk Amsen, Christopher C. Dascher, Bernard Ryffel, Joel A. Swanson, Michael Müller, and J. Magarian Blander. 2011. "Detection of Prokaryotic MRNA Signifies Microbial Viability and Promotes Immunity." *Nature* 474 (7351): 385–89. https://doi.org/10.1038/nature10072.

Shechter, David, Holger L Dormann, C David Allis, and Sandra B Hake. 2007. "Extraction, Purification and Analysis of Histones." *Nature Protocols* 2 (6): 1445–57. https://doi.org/10.1038/nprot.2007.202.

Sloan, Katherine E., Markus T. Bohnsack, and Nicholas J. Watkins. 2013. "The 5S RNP Couples P53 Homeostasis to Ribosome Biogenesis and Nucleolar Stress." *Cell Reports* 5 (1): 237–47. https://doi.org/10.1016/j.celrep.2013.08.049.

Stare, Tjaša, Katja Stare, Wolfram Weckwerth, Stefanie Wienkoop, and Kristina Gruden. 2017. "Comparison between Proteome and Transcriptome Response in Potato (Solanum Tuberosum L.) Leaves Following Potato Virus Y (PVY) Infection." *Proteomes* 5 (3): 14. https://doi.org/10.3390/proteomes5030014.

Starokadomskyy, Petro, Nathan Gluck, Haiying Li, Baozhi Chen, Mathew Wallis, Gabriel N. Maine, Xicheng Mao, et al. 2013. "CCDC22 Deficiency in Humans Blunts Activation of Proinflammatory NF-KB Signaling." *The Journal of Clinical Investigation* 123 (5): 2244–56. https://doi.org/10.1172/JCI66466.

Subramanian, Karthik, Daniel R. Neill, Hesham A. Malak, Laura Spelmink, Shadia Khandaker, Giorgia Dalla Libera Marchiori, Emma Dearing, et al. 2019. "Pneumolysin Binds to the Mannose Receptor C Type 1 (MRC-1) Leading to Anti-Inflammatory Responses and Enhanced Pneumococcal Survival." *Nature Microbiology* 4 (1): 62. https://doi.org/10.1038/s41564-018-0280-x.

Thimmulappa, Rajesh K., Hannah Lee, Tirumalai Rangasamy, Sekhar P. Reddy, Masayuki Yamamoto, Thomas W. Kensler, and Shyam Biswal. 2016. "Nrf2 Is a Critical Regulator of the Innate Immune Response and Survival during Experimental Sepsis." *The Journal of Clinical Investigation* 116 (4): 984–95. https://doi.org/10.1172/JCI25790.

Tweten, Rodney K. 2005. "Cholesterol-Dependent Cytolysins, a Family of Versatile Pore-Forming Toxins." *Infection and Immunity* 73 (10): 6199–6209. https://doi.org/10.1128/IAI.73.10.6199-6209.2005.

Walker, J. A., R. L. Allen, P. Falmagne, M. K. Johnson, and G. J. Boulnois. 1987. "Molecular Cloning, Characterization, and Complete Nucleotide Sequence of the Gene for Pneumolysin, the Sulfhydryl-Activated Toxin of Streptococcus Pneumoniae." *Infection and Immunity* 55 (5): 1184–89.

Will, Cindy L., Henning Urlaub, Tilmann Achsel, Marc Gentzel, Matthias Wilm, and Reinhard Lührmann. 2002. "Characterization of Novel SF3b and 17S U2 SnRNP Proteins, Including a Human Prp5p Homologue and an SF3b DEAD-box Protein." *The EMBO Journal* 21 (18): 4978–88. https://doi.org/10.1093/emboj/cdf480.

Wilson, Boris G., and Charles W. M. Roberts. 2011. "SWI/SNF Nucleosome Remodellers and Cancer." *Nature Reviews Cancer* 11 (7): 481–92. https://doi.org/10.1038/nrc3068.

Wilson, Claire L., and Crispin J. Miller. 2005. "Simpleaffy: A BioConductor Package for Affymetrix Quality Control and Data Analysis." *Bioinformatics (Oxford, England)* 21 (18): 3683–85. https://doi.org/10.1093/bioinformatics/bti605.

841 Wiśniewski, Jacek R., Alexandre Zougman, Nagarjuna Nagaraj, and Matthias Mann.
842   2009. "Universal Sample Preparation Method for Proteome Analysis." *Nature*
843   *Methods* 6 (5): 359–62. https://doi.org/10.1038/nmeth.1322.
844 Zafar, M. Ammar, Yang Wang, Shigeto Hamaguchi, and Jeffrey N. Weiser. 2017.
845   "Host-to-Host Transmission of Streptococcus Pneumoniae Is Driven by Its
846   Inflammatory Toxin, Pneumolysin." *Cell Host & Microbe* 21 (1): 73–83.
847   https://doi.org/10.1016/j.chom.2016.12.005.
848 Zahlten, Janine, Ye-Ji Kim, Jan-Moritz Doehn, Thomas Pribyl, Andreas C. Hocke,
849   Pedro García, Sven Hammerschmidt, Norbert Suttorp, Stefan Hippenstiel,
850   and Ralf-Harto Hübner. 2015. "Streptococcus Pneumoniae–Induced Oxidative
851   Stress in Lung Epithelial Cells Depends on Pneumococcal Autolysis and Is
852   Reversible by Resveratrol." *The Journal of Infectious Diseases* 211 (11):
853   1822–30. https://doi.org/10.1093/infdis/jiu806.
854 Zhao, Hailin, Shiori Eguchi, Azeem Alam, and Daqing Ma. 2017. "The Role of
855   Nuclear Factor-Erythroid 2 Related Factor 2 (Nrf-2) in the Protection against
856   Lung Injury." *American Journal of Physiology - Lung Cellular and Molecular*
857   *Physiology* 312 (2): L155–62. https://doi.org/10.1152/ajplung.00449.2016.
858

859 **Figure legends:**

860 **Figure 1: *S. pneumoniae* induced differential gene expression.**

861 Monocyte derived macrophages (MDMs) were challenged with either *S. pneumoniae*,

862 the isogenic pneumolysin negative mutant (ΔPLY) or mock infected with phosphate

863 buffered saline (MI) in biological replicates of three. After 3 h incubation the gene

864 expression was measured using Affymetrix arrays. A) volcano plots comparing log2

865 (fold change) to log10 p value for MI vs *S. pneumoniae* challenged MDMs. B) volcano

866 plots comparing log2 (fold change) to log10 p value for MI vs ΔPLY challenged MDMs.

867 C) volcano plots comparing log2 (fold change) to log10 p value for *S. pneumoniae* vs

868 ΔPLY challenged MDMs. The probe-sets in blue have a p value <0.05, in red an

869 adjusted p value <0.05 (following FDR correction) and in green an adjusted p value

870 <0.05 and an absolute fold change greater than 1.

871
872 **Figure 2: Oxidative stress response pathway terms significantly upregulated.**

873 Monocyte derived macrophages (MDMs) were challenged with either *S. pneumoniae*,

874 the isogenic pneumolysin negative mutant (ΔPLY) or mock infected with phosphate

875   buffered saline (MI) in biological replicates of three. After 3 h the gene expression was

876   measured using Affymetrix arrays. A) volcano plots comparing log2 (fold change) to

877   log10 p value for MI vs *S. pneumoniae* challenged MDMs. B) volcano plots comparing

878   log2 (fold change) to log10 p value for MI vs ∆PLY challenged MDMs. The highlighted

879   genes belong to the Oxidative stress response Gene Ontology term and are

880   significantly expressed (q value <0.05). In red are those found in challenge with both

881   strains, in blue the genes that are only found in the response to ∆PLY challenge and

882   in orange the pneumolysin-dependent genes found after *S. pneumoniae* but not ∆PLY.

883

884   **Fig 3: Pneumolysin is responsible for changes in relative abundance of PTMs**

885   **on histone H3.**

886   Monocyte derived macrophages (MDMs) were challenged with either *S.*

887   *pneumoniae*, the isogenic pneumolysin negative mutant (∆PLY) or mock infected

888   with phosphate buffered saline (MI) in biological replicates of three. After 3 h

889   incubation the histones were extracted and analysed by mass spectrometry and the

890   relative abundance of each post translational modification (PTM) was measured for

891   each peptide. The bar plots represent the relative abundance of each PTM

892   quantified, blue represents the abundance in MI MDMs, green following challenge

893   with *S. pneumoniae* and in red to ∆PLY. A) Peptide TKQTAR shows an increase in

894   the level of H3K4me1. B) Peptide KSTGGKAPR shows a decrease in the level of

895   H3K9me2 in a pneumolysin-dependent manner. C) Peptide KQLATKAAR shows a

896   relative increase in the level of H3K23ac in response to both bacterial challenges. D)

897   Peptide KSAPATGGVKKPHR shows a decrease in H3K27me2 following challenge

898   with *S. pneumoniae* compared to MI, an increase in the level of H3K27me2K36me2

899   and a reciprocal drop in H3K27me3K36me1 in response to ∆PLY challenge

35

900   compared to MI. E) Peptide EIAQDFKTDLR shows an increase in the relative

901   abundance of H3K79me2 following challenge with ∆PLY. F) Peptide

902   KSAPSTGGVKKPHR of H3.3 shows an increase in H3.3K36me2 and in

903   H3.3K27me2K36me1 with a reciprocal drop in H3.3K27me2K36me2. (One-way

904   ANOVA, * p<0.05, ** p<0.01, *** p<0.001, error bars represent mean and standard

905   deviation).

906
907   **Fig 4: Pneumolysin is responsible for changes in relative abundance of PTMs**

908   **on histone H4.**

909   Monocyte derived macrophages (MDMs) were challenged with either *S.*

910   *pneumoniae*, the isogenic pneumolysin negative mutant (∆PLY) or mock infected

911   with phosphate buffered saline (MI) in biological replicates of three. After 3 h

912   incubation the histones were extracted and analysed by mass spectrometry and the

913   relative abundance of each post translational modification (PTM) was measured for

914   each peptide. The bar plots represent the relative abundance of each PTM

915   quantified, blue represents the abundance in MI MDMs, green following challenge

916   with *S. pneumoniae* and in red to ∆PLY. A) Peptide GKGGKGLGKGGAKR shows a

917   relative increase in the level of H4K16ac following challenge with *S. pneumoniae* in

918   comparison to the ∆PLY. B) Peptide KVLR shows a decrease in the level of

919   H4K20me2 in a pneumolysin-dependent manner compared and a reciprocal

920   increase in the H4K20me1. Conversely for the MDM challenged with ∆PLY there

921   was a rise in H4K20me2 and a fall in the level of H4K20me1.(n=3. One way ANOVA,

922   * p<0.05, ** p<0.01, *** p<0.001, **** p<0.0001).

923
924   **Fig 5: Pneumolysin leads to blunted TNFα release by repressing mRNA**

925   **production.**

926   Monocyte derived macrophages (MDMs) were challenged with either *S. pneumoniae*,

927   the isogenic pneumolysin negative mutant (ΔPLY), the isogenic pneumolysin negative

928   mutant with reconstituted pneumolysin (PLY-ΔPLY). or mock-infected with phosphate

929   buffered saline (MI). A) After 3 h incubation RNA was extracted from MDMs and RT-

930   qPCR performed to measure the abundance of TNFα mRNA. The Bar chart

931   represents the $\Delta\Delta$CT fold change for each bacterial challenge demonstrating

932   significantly higher abundance of TNFα mRNA following challenge with ΔPLY. One-

933   way ANOVA F statistic =0.01 and p value <0.05. B) At 3 h TNFα concentration were

934   measured in the supernatants of MDMs challenged with each strain. The Bar chart

935   demonstrate the significantly raised level of TNFα in response to challenge with ΔPLY

936   (n=8, one way ANOVA F statistic = 0.0011, p<0.05). C) TNFα and IL-6 cytokines were

937   measured in supernatants following challenge with *S. pneumoniae* or ΔPLY at 0.5, 1,

938   2, 3, 4, 5, 6, 7 h. The bar charts represent mean and Standard Deviation of 3 biological

939   replicates run in technical duplicates are shown demonstrating a significant difference

940   in the rise of TNF-α between the two strains at 4 h, (black line highlights differences

941   between control and ΔPLY, red line between control and *S pneumoniae*, blue line *S*

942   *pneumoniae*, and ΔPLY, * p<0.05, ** p<0.01, **** p<0.0001).

943

944   **Fig 6: The HDAC inhibitor Vorinostat suppresses TNFα levels to similar levels**

945   **as pneumolysin.**

946   Monocyte derived macrophages (MDMs) were challenged with either *S. pneumoniae*,

947   the isogenic pneumolysin negative mutant (ΔPLY) or mock infected with phosphate

948   buffered saline (MI) in the presence of 3 μM vorinostat (SAHA) or vehicle control (0.5%

949   DMSO). The Bar chart and standard deviation represents the levels of TNFα in the

950   supernatants demonstrating that suppression of TNFα can be mimicked by SAHA to

951   similar levels as in the presence of PLY. (n=7 p<0.05).

952

953   **Supplementary Figure legends:**

954   **Fig S1: Viable intracellular bacteria following 3 h challenge with *S. pneumoniae*,**

955   **ΔPLY or PLY-ΔPLY mutants.**

956   Monocyte derived macrophages (MDMs) were challenged with either *S. pneumoniae*,

957   the isogenic pneumolysin negative mutant (ΔPLY) or the isogenic pneumolysin

958   negative mutant with reconstituted pneumolysin (PLY-ΔPLY). At 3 h the number of

959   viable intracellular bacteria was determined. The results are expressed as mean and

960    $\log_{10}$ of cfu/mL and represented as bar chart with standard deviation. (n=3, one way

961   ANOVA p=0.99)

962

963   **Fig S2: Heatmap of the differentially expressed probes following MDM**

964   **challenge.**

965   Monocyte derived macrophages (MDMs) were challenged with either *S. pneumoniae*,

966   the isogenic pneumolysin negative mutant (ΔPLY) or mock-infected with phosphate

967   buffered saline (MI) in biological replicates of three. At 3 h the gene expression was

968   measured using Affymetrix arrays. This heatmap represents genes found to be

969   differentially expressed (one-way ANOVA, with F p value <0.05).

970

971   **Fig S3: Gene ontology biological processes enriched terms show stress**

972   **responses and metabolism are over-represented.**

973   Monocyte derived macrophages (MDMs) were challenged with either *S. pneumoniae*,

974   the isogenic pneumolysin negative mutant (ΔPLY) or mock-infected with phosphate

975   buffered saline (MI) in biological replicates of three. At 3 h the gene expression was

976 measured using Affymetrix arrays. The bubble plot shows the top ten enriched Gene

977 Ontology (GO) biological processes terms in both the pneumolysin mutant and the

978 parental strain analysis. The bubble size and colour correspond to the number of

979 genes which have mapped to the GO term. The bubbles are plotted along the x axis

980 according to the –log10 p value for the enrichment.

981

982 **Table S1: Canonical pathway analysis of up-regulated differentially expressed**

983 **probes following challenge of MDMs with *Streptococcus pneumoniae* using**

984 **XGR.**

985 **Table S2: Canonical pathway analysis of up-regulated differentially expressed**

986 **probes following challenge of MDMs with ∆PLY using XGR**

TNFα cytokine level

Figure 6

a) GKGGKGLGKGGAKR

b) KVLR
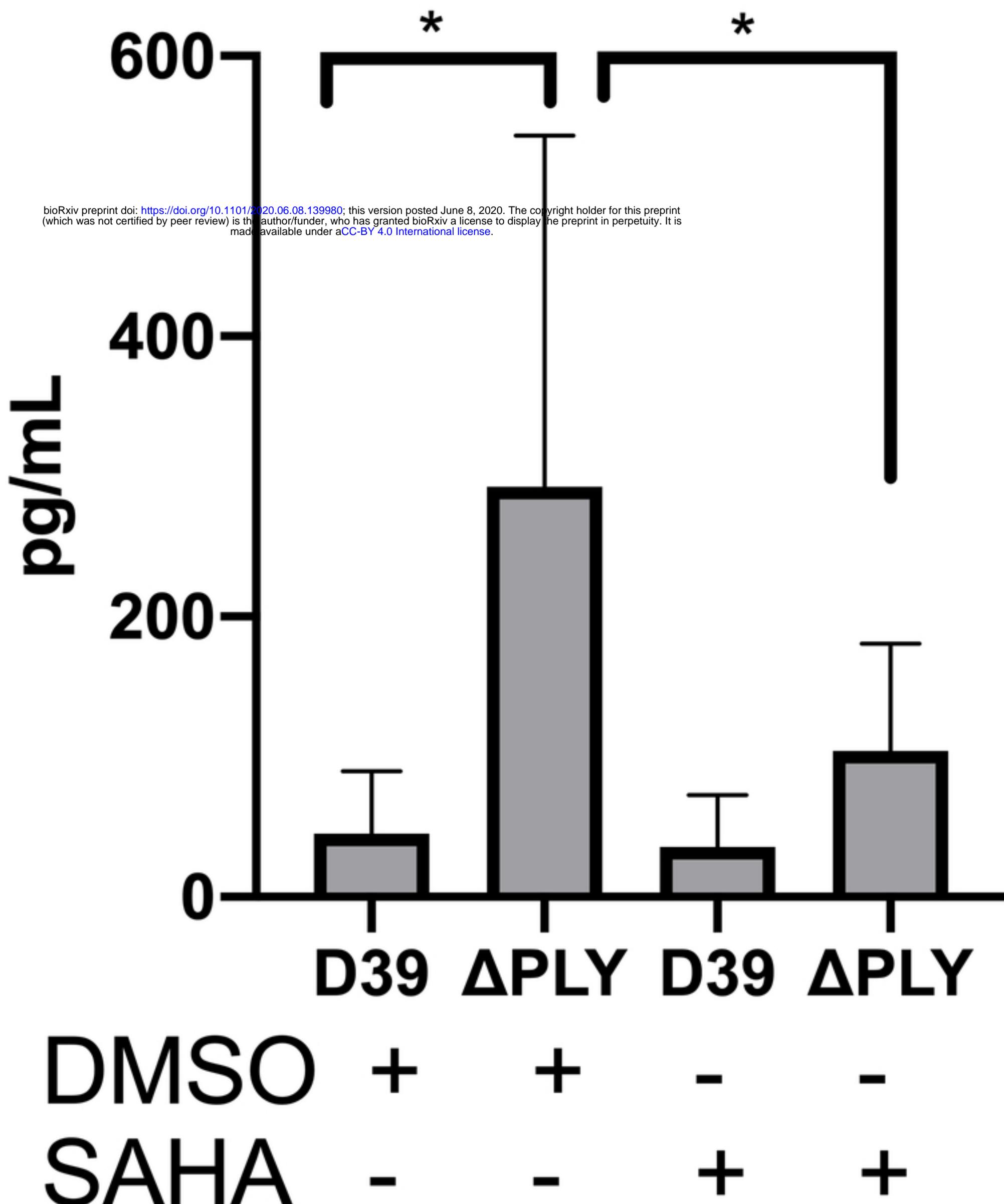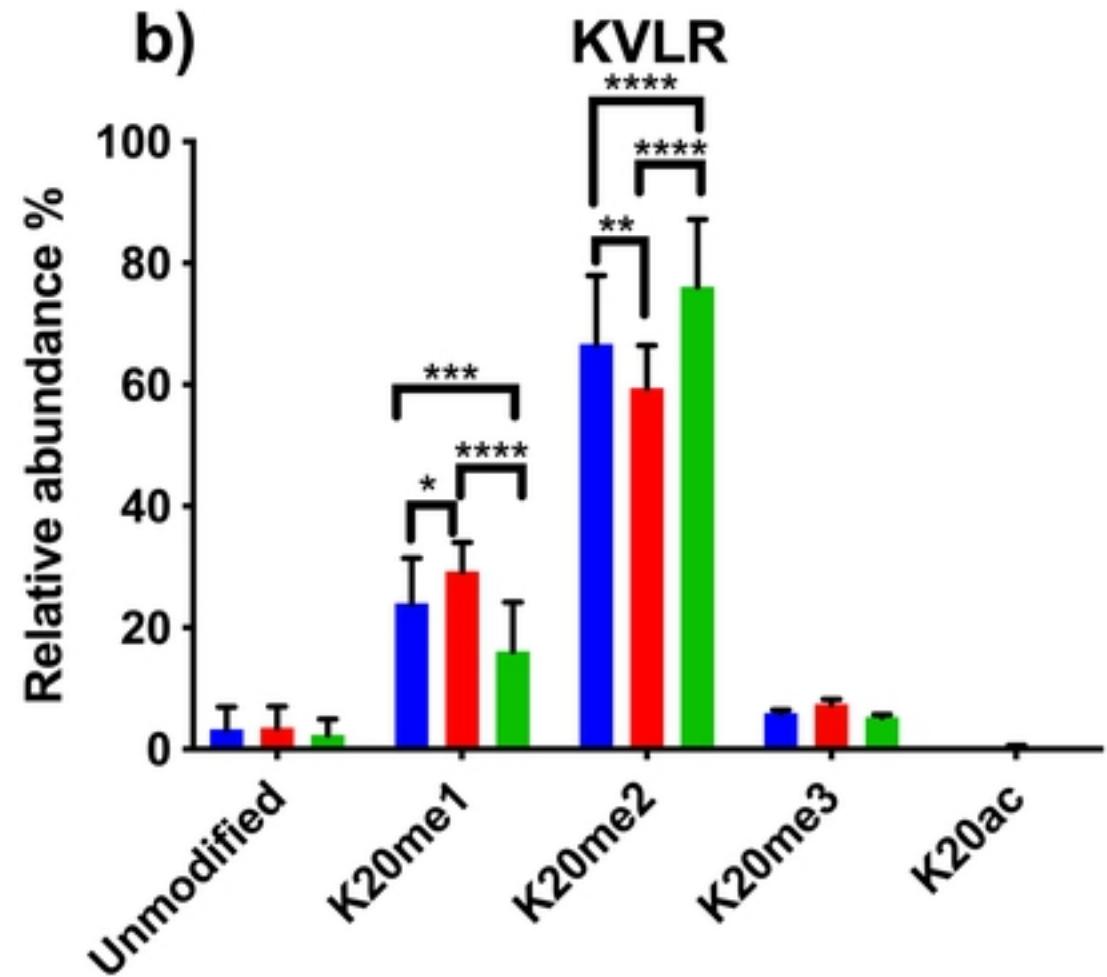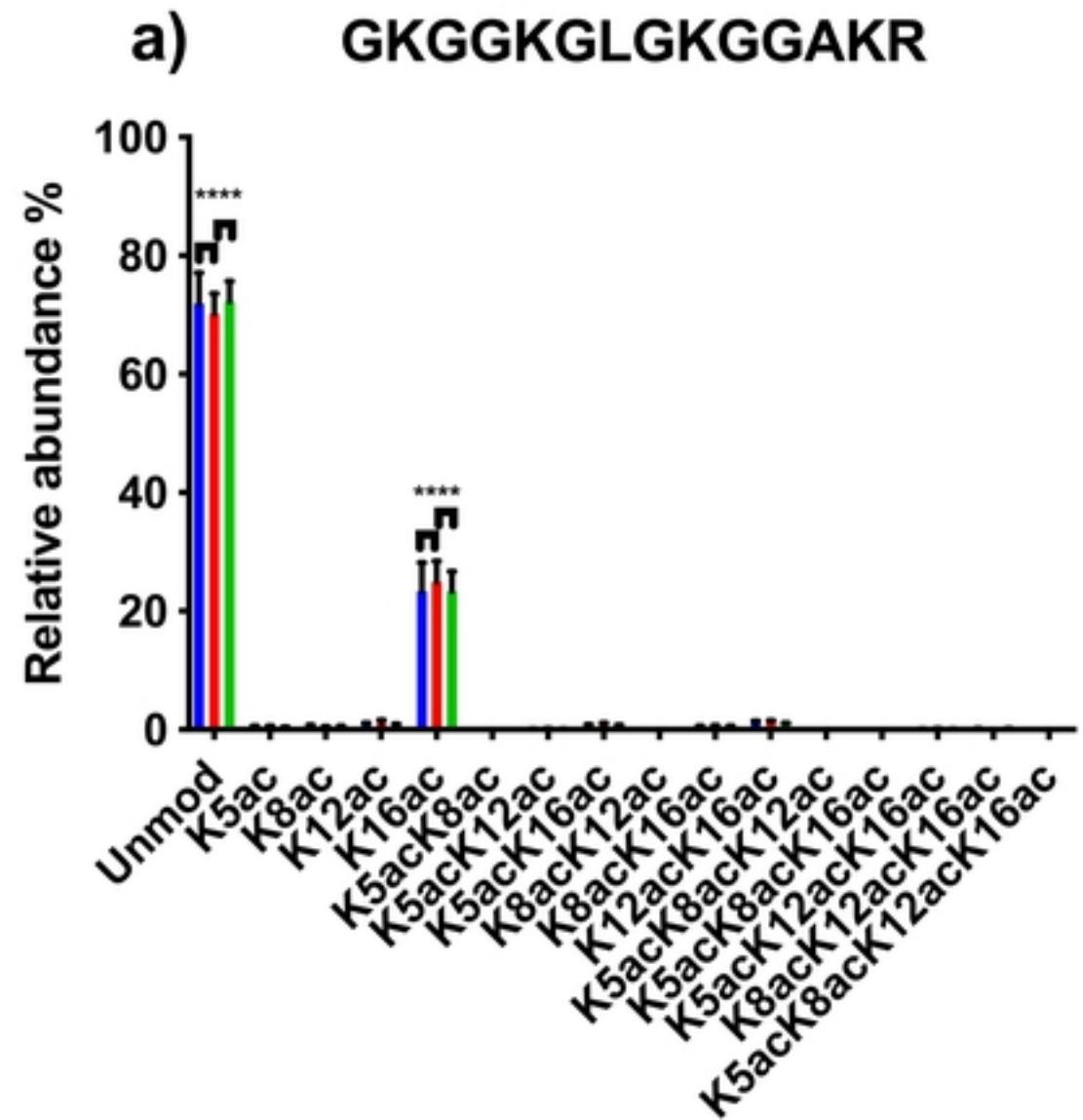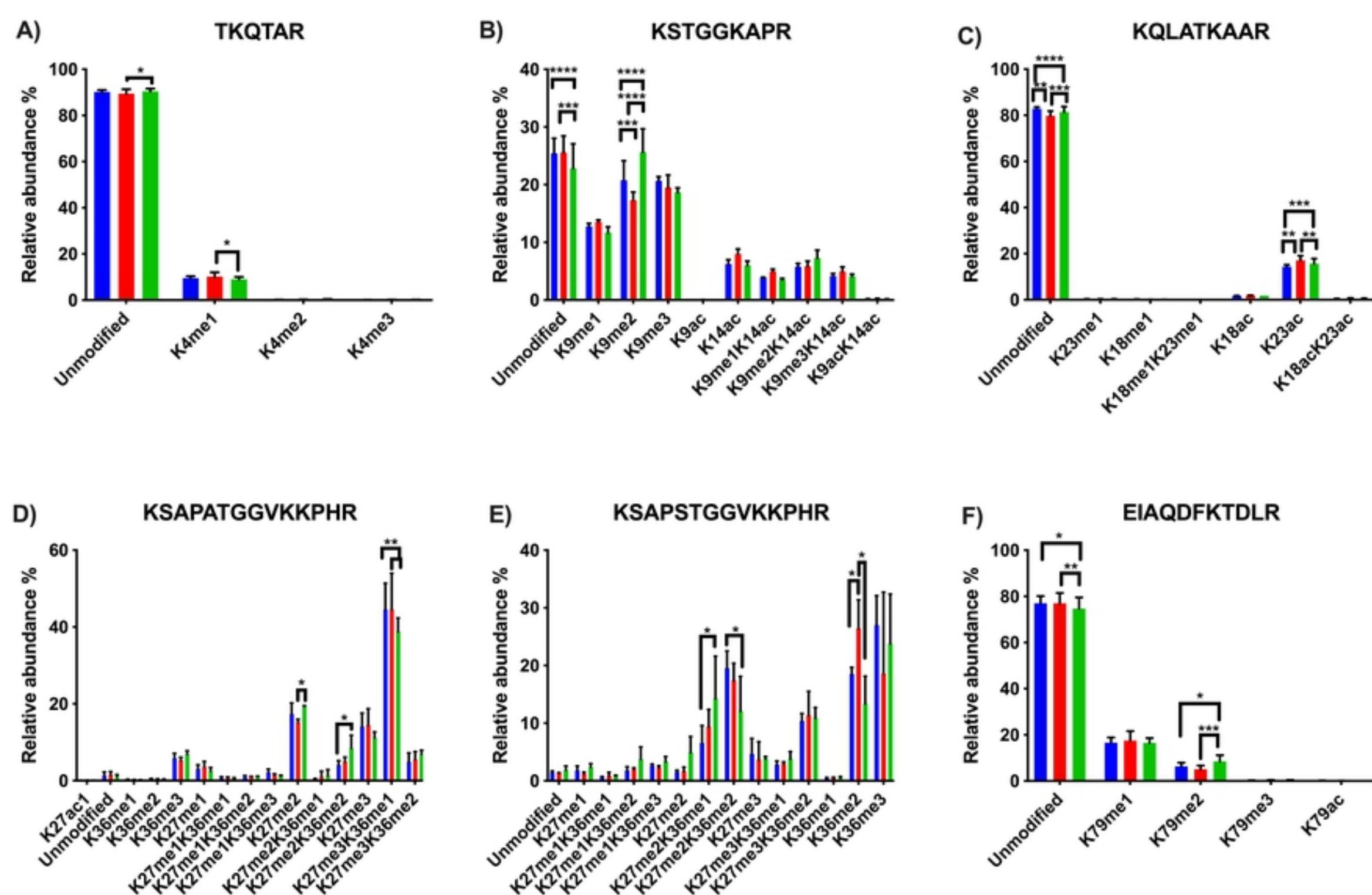
Figure 4

Figure 3

Figure 2

Figure 1

A) TNFα mRNA

B) TNFα cytokine level

C) IL-6 production / TNF α

n=6 F=0.01 p=0.03

n=8 F=0.0011

S. pneumoniae
ΔPLY

Figure 5